Inkjet Printed Flexible Non-Enzymatic Glucose Sensor for Tear Fluid Analysis

Agostino Romeo,[a,b] Ana Moya,[c,d] Tammy S. Leung,[a,c,†] Gemma Gabriel,[c,d] Rosa Villa,[c,d] Samuel Sánchez[a,b,e,*]

[a] Smart Nano-Bio-Devices Group, Institute for Bioengineering of Catalonia (IBEC), The Barcelona Institute of Science and Technology (BIST), Barcelona, Spain
[b] Max Planck Institute for Intelligent Systems, Stuttgart, Germany
[c] Instituto de Microelectrónica de Barcelona, IMB-CNM (CSIC), Esfera UAB, Campus Universitat Autonoma de Barcelona, Bellaterra, Barcelona, Spain
[d] Research Networking Center in Bioengineering, Biomaterials and Nanomedicine (CIBER-BBN), Barcelona, Spain
[e] Institució Catalana de Recerca i Estudis Avancats (ICREA), Barcelona, Spain

ARTICLE INFO

Keywords:
Inkjet printing
Non-enzymatic sensor
Glucose
Copper oxide
Tear analysis

ABSTRACT

Here we present a flexible and low-cost inkjet printed electrochemical sensor for enzyme-free glucose analysis. Versatility, short fabrication time and low costs make inkjet printing a valuable alternative to traditional sensor manufacturing techniques. We fabricated electro-chemical glucose sensors by inkjet printing electrodes on a flexible polyethylene terephthalate substrate. CuO microparticles were used to modify our electrodes, leading to a sensitive, stable and cost-effective platform for non-enzymatic detection of glucose. Selectivity, reproducibility, and life-time provided by the CuO functionalization demonstrated that these sensors are reliable tools for personalized diagnostics and self-assessment of an individual's health. The detection of glucose at concentrations matching that of tear fluid allows us to envisage applications in ocular diagnostics, where painless and non-invasive monitoring of diabetes can be achieved by analyzing glucose contained in tears.

1. Introduction

Compact biosensors have a huge potential in clinical diagnostics and health self-assessment as they easily and quickly measure diagnostically-relevant bioanalytes.[1] Performing analysis without expensive and time-consuming techniques, like those hosted in specialized hospital structures, relies on innovative sensing platforms with lower cost and higher adaptability. To achieve this goal, sensor manufacturing techniques alternative to traditional ones, like photolithography and screen printing, are object of investigation. For instance, inkjet printing (IJP) has recently emerged as a promising platform for rapid, adaptable and cost-effective fabrication of sensors.[2,3] IJP has several advantages over traditional manufacturing methods, such as: i) high versatility, because no masks or stencils are needed to pattern conductive paths on a substrate, which makes this entire technology extremely application-tailorable; ii) low cost, because no expensive facilities are required and printing materials are efficiently employed only where needed; iii) short fabrication time and high scalability; and iv) contact-less fabrication, which prevents contamination and damage of the substrate. Moreover, fabrication of electronic devices on flexible plastic substrates creates new opportunities when conformability to or implantability in our body is required, while keeping weight and cost of the final devices low.[4–7] In fact, IJP is well suited for the fabrication of sensors on flexible substrates, which permits to obtain conformable devices that can be worn and used for personalized health assessment. As a whole, these features make IJP technology an ideal candidate both for rapid prototyping and large-scale production of biological and chemical sensors.

Enzymatic detection is one of the most widespread transduction mechanisms in biosensing.[8] However, the use of enzymes presents several challenges, namely their poor reproducibility, long-term stability and the strong dependence of their activity on temperature and pH.[9] On the contrary, enzyme-free sensors show enhanced stability, simplicity, reproducibility, and cost effectiveness.[10] A plethora of electrocatalysts have been

described for non-enzymatic sensing.[11,12] Among them, copper and cupric oxide (CuO) are of special interest for the non-enzymatic detection of glucose.[13,14] CuO, for instance, is earth-abundant and cheaper than noble metal nanoparticles (Au, Pt, Pd, etc.), which are also often used as catalytic materials in non-enzymatic glucose sensors.[14] Moreover, copper and Cu-oxides have high electrocatalytic activity and strong resistance to poisoning species, such as chloride ions (Cl^-), that are known to seriously degrade the properties of noble metals.[15]

Blood is the main body fluid used for diagnostic purposes, although blood-related analysis suffers several drawbacks, such as blood sampling in hemophobic patients, possible sensitization or infection of the blood sampling areas and challenging continuous monitoring. On the other hand, biochemical analysis of external body fluids (e.g., sweat, saliva, tear fluid, urine, etc.) has recently attracted considerable interest in Point-of-Care (PoC) diagnostics,[16–18] as this permits non-invasive and pain-less procedures.[19] Among other external body fluids, tear fluid has a high potential for non-invasive diagnostics, due to its rich composition in glucose, electrolytes, proteins, etc.[20,21] Several examples of tear sensors have been reported in the literature, mainly aimed at enzymatically measuring glucose levels.[22–24] As monitoring of glucose has vast medical utility for diabetes treatment, the development of innovative glucose sensors is an urgent asset in biomedical research.

In this work, we describe a sensitive non-enzymatic glucose sensor fabricated by the rapid and cost-effective IJP technique on flexible substrates using low curing-temperature inks. We demonstrate that, upon modification with CuO microparticles (CuO-µPs), our sensor can detect glucose at concentrations appropriate for tear fluid analysis. Versatile fabrication, full integration of the sensor electrodes and remarkable sensing performance make our sensor particularly well suited for non-invasive and painless PoC diagnostics.

2. Experimental section

2.1. Chemical and reagents

A low-curing temperature ink based on gold nanoparticles (DryCure-Au) was purchased from C-Ink, Japan, a silver nanoparticle ink (PE410) was purchased from DuPont, Korea, and an SU8 ink (2002) was purchased from MicroChem, USA. Polyethylene Terephthalate (PET) films (MELINEX ST 504) with a thickness of 125 µm was purchased from DuPont Teijin Films. Copper(II) nitrate pentahydrate (10699) and ethylenediamine (EDA, A12132) were purchased from Alfa Aesar, Spain. Hydrazine hydrate (225819), sodium hydroxide (30620), poly-vinylpyrrolidone MW = 10,000 (PVP10), ethanol, and nafion (70160) were purchased from Sigma-Aldrich, Spain. Milli-Q water (18.6 MΩ) was used to prepare all aqueous solutions. All chemicals were used without further purification.

2.2. Inkjet printing process

A piezoelectric Dimatix Material Printer (DMP-2831 from FUJIFILM-Dimatix, Inc., USA) was used for the inkjet printing of the sensors on flexible PET substrates. The cartridges used for printing were user-fillable 10 pL nominal drop volume printheads having 16 nozzles each with a diameter of 21.5 µm. Printing patterns were designed using Electronic Design Automation layout software and imported into the Dimatix Bitmap editor software. The substrate vacuum plate was temperature controllable. The piezoelectric nozzle voltages were optimized before each print run and for each ink, being generally on the order of 18-20 V for gold ink, 27-30 V for silver ink and 19-20 V for SU8 ink, at a printing frequency of 5 kHz for all the inks used. The printing processes were carried out in a standard laboratory environment in ambient condition, without non-particulate filtered enclosure systems and control of temperature or humidity. The low-curing temperature gold ink was employed to print working electrode (WE) and counter electrode (CE). The silver ink was used to print reference electrode (RE), interconnects and pads. The passivation of the tracks was done using the SU8 ink. The diameter of the

working electrode is 3 mm. The sensors were designed to be connected to a potentiostat using a zero-insertion force (ZIF) connector (Molex, Spain).

2.3. Synthesis and characterization of CuO-µPs

CuO-µPs were obtained upon oxidation of a water dispersion of copper nanowires (Cu-NWs) prepared following a protocol reported by B.J. Wileys and co-workers.[25] Briefly, a solution composed of 20 mL NaOH 15M**,** 1mL $Cu(NO_3)_2$ 0.1M + 150 µL EDA + 25 µL hydrazine 35% wt was prepared in a round bottom flask. This solution was heated at 80 °C and stirred at 250 rpm for 1 hour. When the solution cooled down, it was centrifuged at 4500 rpm (1480 g) for 5 minutes. The supernatant was removed and the pellet re-dispersed in 5mL hydrazine 3% wt. Seven washing steps in hydrazine 3% wt were done to eliminate unreacted residuals, then the as-prepared Cu-NWs were finally resuspended in Milli-Q water. The reddish-brown water dispersion of Cu-NWs was stored at room temperature for future use. Oxidation of copper during storage in water takes place, resulting in a grey-black dispersion made of CuO-NWs with micrometric bumps and excrescences on their surface. Brittle CuO-NWs fragment upon mechanical stress induced by shaking or pipetting, and release the excrescences as micrometric particles. The copper-based material used to functionalize the sensors in this work consists of a dispersion of these CuO-µPs. The morphology of the copper-based samples was investigated by Scanning Electron Microscopy (SEM) using a DSM 982 Gemini high resolution SEM (Zeiss) equipped with a Schottky-Emitter (5 kV operating voltage). The chemical composition of the copper-based samples was analyzed by Energy Dispersive X-ray (EDX) using a Silicon Drift Detector Ultradry cooled via peltier cooling mounted on the SEM.

2.4. Electrode modification and measurements

Gold WE modified with CuO-µPs were prepared by drop-casting 35 µL of a 5 µg/mL Cu-based solution (0.17 µg) on the surface of the WE, drying at room temperature, and then drop-casting 3 µL Nafion solution in ethanol (0.1%, V/V) for microparticle immobilization. The Au/CuO-µPs/Nafion WE is hereafter indicated as modified WE. The printed silver pseudo-reference electrode of each sensor was chlorinated before testing by exposing it to concentrated sodium hypochlorite for 5 seconds. Electrochemical measurements were performed using an Autolab PGSTAT 204 potentiostat/galvanostat (EcoChemie, The Netherlands) controlled by a personal computer. ZIF connectors were used to connect the sensors to the potentiostat, resulting in a cost- and time-efficient solution that enables reusability and easy interchange of devices. Cyclic voltammetry (CV) was performed by sweeping the potential between -0.2 V and +0.8 V at scan rate in the range 10 - 200 mV s^{-1}, unless otherwise specified in the text. The chronoamperometry (CA) measurements were performed by applying a constant potential vs. Ag/AgCl printed RE. Both CV and CA measurements were carried out in 2 mL of 0.1 M NaOH electrolyte under ambient conditions while stirring at 150 rpm. All the experiments were repeated at least three times to verify reproducibility.

2.5. Measurements on human tear fluid

Tearing was stimulated by onion vapor 30 min after a meal. The tear fluid generated was collected using glass capillaries (VitroCom, New Jersey, USA) with internal diameter of 0.6 mm.

3. Results and discussion

3.1. Sensors design and fabrication

The fabrication route of the IJP glucose sensor is shown in Fig. 1A. First, the sensors were designed using a layout editor to match the required geometrical needs for a given application (Fig. 1A, a). All inks were printed on flexible PET films, used as an archetypal substrate to show the suitability to the IJP for flexible electronics. Prior to beginning the printing step (Fig. 1A, b), silver, gold and SU8 inks' behaviour were studied by printing a

predefined line pattern over the PET substrate.[26] This test print pat-tern allowed us to optimize some critical parameters, such as the drop spacing (DS) required to print a continuous line, as well as the thickness and width of the line. These parameters depend on the final surface energy of each ink on the desired substrate, hence this is a mandatory step before each printing. In the first step of the printing (Fig. 1A, b1) the WE and CE were printed with the gold ink using a 15 µm DS. Subsequently, interconnects and pads were printed using the silver ink with a 30 µm DS (Fig. 1A, b2). During the printing of both conductive inks, the substrate temperature was set to 40 °C to promote a first partial evaporation of the inks solvents and to increase the pattern resolution. To achieve a complete removal of all solvent molecules absorbed on the ink nanoparticles, a drying step is necessary (Fig. 1A, b3). This was optimized at 100 °C for 10 min. Next, a sintering step is necessary to achieve a low resistivity of the inks. Although higher temperatures can achieve better conductivities, a sintering step of 20 min at 130 °C was enough to achieve resistivity down to 80 µΩ·cm. It is important to highlight the careful selection of the inks to ensure full compatibility with low temperature processing, that allows the exploitation of low-cost plastic substrates. Finally, an SU8 passivation layer was printed over the interconnects with a 15 µm DS (Fig. 1A, b4), leaving uncovered the sensing area (WE, CE, RE) and the pad connections. The photoresist SU8 achieves a high chemical resistance and thermal stability after a soft bake at 100ºC for 5 min and a UV curing of 15 seconds during which the layer polymerizes by cross-linking (Fig. 1A, b5).

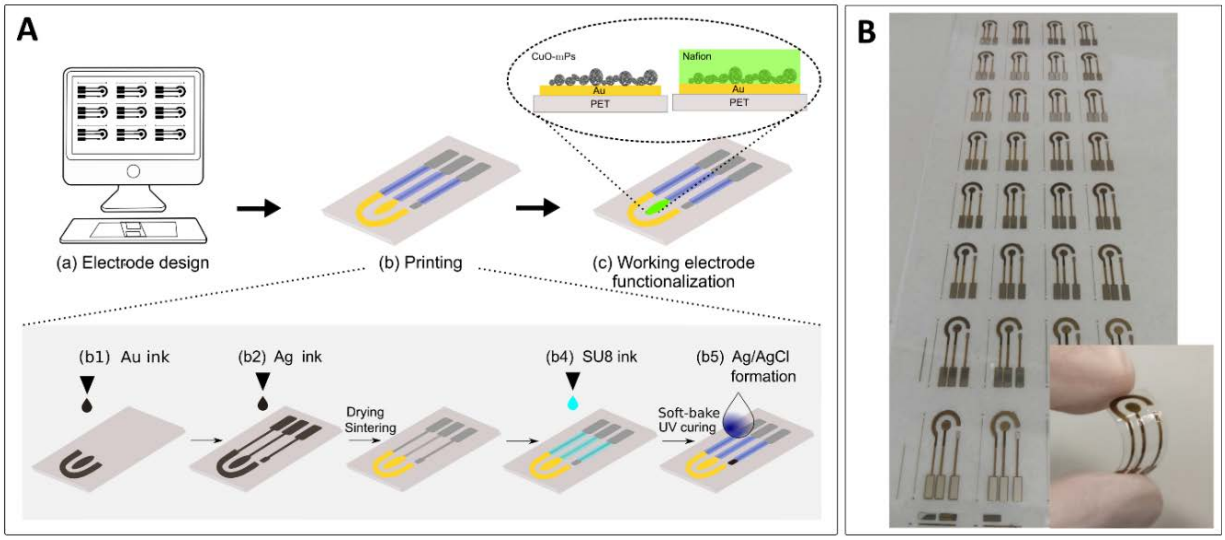

Figure 1. IJP sensors for non-enzymatic glucose detection. A) Schematic representation of the device fabrication and structure: (a) Sensor layout is designed using a layout software and sent to the inkjet printer; (b) sensors are inkjet printed onto a flexible PET substrate using inks based on gold nanoparticles for WE and CE, on silver nanoparticles for RE, interconnects and pads, and on SU8 for the passivation layer over the interconnects; (c) WE was functionalized using CuO-µPs and Nafion. B) Photographs of a series of sensors printed on an A4 PET sheet, showing the mass production scalability of the inkjet printing method described here. Inset: picture of a bended IJP sensor showing good flexibility. Total size of each IJP sensor: 25 x 9 mm^2.

It is worth to note that a little potential shift exists in electrochemical sensors when integrated printed RE are used instead of external RE. This was confirmed by CV measurements on a pair of IJP gold WE and CE, where the printed RE was compared to an external Ag/AgCl, saturated 3 M KCl (Metrohm, The Netherlands), using a 0.1 M KCl, 0.01 M PBS, 5 mM Fe(CN6)3-/4- solution as the electrolyte (Figure S1). The little potential shift (around 100 mV) can be attributed to the difference of chloride concentration in contact with the electrode (printed RE: 0.1 M, inter-nal solution of the external RE: 3 M). Once the printing was complete, the gold WE was functionalized

with CuO-µPs by drop casting. Finally, Nafion was used as an immobilizing layer to firmly anchor the CuO-µPs to the electrode surface. Polymeric binders may limit the charge transfer at the electrode and increase the ion diffusion resistance at the electrode/electrolyte interface, hence decreasing the overall electroactivity of the system. In order to prevent these common drawbacks resulting from covering electrodes with polymer matrix, a very low concentration of Nafion (0.1%) was used. Fig. 1B shows a picture of a single device, and the flexibility of the PET substrate. The mass fabrication of these devices in an A4 sheet PET size is possible, which can be achieved in approximately 3 hours. The final cost of materials for a single IJP sensor was estimated around 0.182 € as shown in Table TS1.

3.2. Characterization of the CuO-µPs

As-prepared nanowires showed an average length of 9.1 ± 1.6 µm and diameter of 320 ± 60 nm (N=10, errors are standard error of the mean) (Fig. S2A). Wires also showed a smooth surface, typical of copper nanomaterials.[27] The pure copper composition of the wires was confirmed by EDX analysis (Fig. S2B), where no specific localization of oxygen could be observed along the nanowires. The peaks corresponding to silicon and oxygen in the EDX spectrum could be accounted for by the native oxide typically found on a silicon wafer (used as the substrate for the SEM and EDX measurements presented here). Storage in water induced oxidation of copper, giving rise to a dispersion of CuO-NWs. Oxidized nanowires show micrometric bumps and excrescences on their sur-face, that are released as CuO-µPs upon mechanical stress induced by shaking or pipetting. This dispersion of CuO-µPs was used to functionalize sensors in this work (Fig. 2A). The copper oxide composition of the micrometric particles was confirmed by EDX analysis (Fig. 2B, C), showing that oxygen is clearly localized on the CuO-µP, thus revealing the oxidized state of copper.

3.3. Optimal operating conditions for glucose detection

The mechanisms underlying the electrochemical kinetics of glucose oxidation can be investigated by CV performed at different scan rates. Fig. 3A shows CV curves measured at scan rates ranging from 10 to 200 mV s^{-1} in the presence of 500 µM glucose. The current of the anodic peak linearly depends on the scan rate (R2 = 0.999), as reported in Fig. 3B. The linear relationship observed indicates that the electro-oxidation process of glucose is driven by adsorption-controlled mechanisms. The performance of electrochemical sensors is affected by several parameters, such as the operating potential applied and, for Cu-based non-enzymatic sensing, the alkalinity of the electrolyte. In order to thoroughly evaluate the performance of our CuO-µPs glucose sensor, we tested it to select the optimal operating conditions. Interestingly, the potential of the anodic peak depends on the concentration of glucose. CV was measured with modified electrodes in 0.1 M NaOH as the electrolyte in the presence of increasing concentrations of glucose, as reported in Fig. 3C (scan rate: 30). A shoulder peak can be seen from 0.3 – 0.55 V, in agreement with the typical glucose oxidation potential. The plot of the anodic peak voltage vs glucose concentration is shown in Fig. 3D, where it can be inferred that working potentials below 0.45 V provide the highest sensitivity to very low glucose concentrations (<500 µM), like those contained in tear fluid. For this reason, we chose a potential V^*_m=0.4 V as the working potential for the CA detection of glucose with modified WE reported in the following. The electro-catalytic oxidation of glucose on CuO- based electrodes directly involves hydroxyl radicals (Fig. 4A) and its efficiency strongly depends on the alkalinity of the system. Thus, to define the optimal concentration of NaOH to effectively support the electro-oxidation of glucose, several CV were measured in the presence of 500 µM glucose and increasing concentrations of NaOH in the 5-200 mM range (scan rate: 30 mV s^{-1}). As reported in Fig. S3, low levels of NaOH generate low signal around 0.4 V, because few hydroxyl radicals are available to sustain the electro-oxidation of glucose. The current of the anodic peak at 0.4 V increases with the NaOH concentration. However, the observed signal increase from 100 mM to

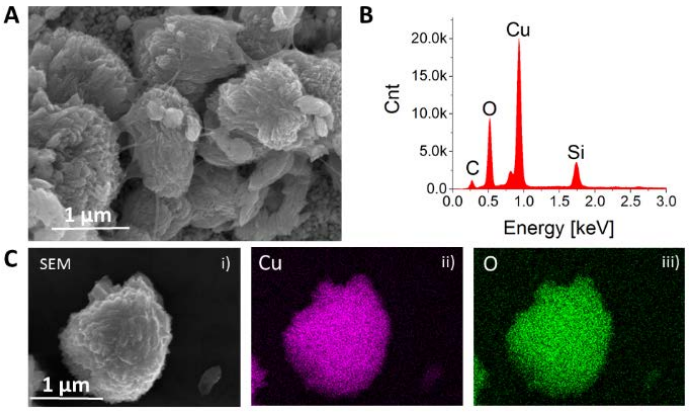

Figure 2. A) Low magnification SEM micrograph of a IJP gold WE functionalized with CuO-µPs. B) EDX spectrum of a CuO-µP. C) i) High magnification SEM image of a CuO-µP, ii) and iii) EDX mappings of Cu and O, respectively.

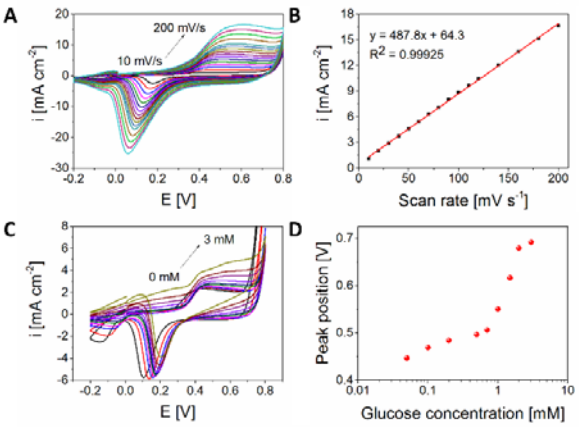

Figure 3. Identification of the optimal working conditions for the electrochemical detection of glucose. A) CV curves of a modified WE measured at scan rates from 10 mV s^{-1} to 200 mV s^{-1} in a 0.1 M NaOH solution supplemented with 500 µM glucose. B) Plot showing the dependence of the anodic peak current on the scan rate. C) CV with modified WE in 0.1 M NaOH as the electrolyte in the presence of 0-3 mM glucose (scan rate: 30 mV s^{-1}). D) Plot of the electro-oxidation potential of glucose as a function of the glucose concentration.

200 mM is not significant, probably due to the high amount of hydroxyl radicals that hinder the electro-catalytic sites on the CuO-µPs. Therefore, 100 mM NaOH was chosen as the electrolyte concentration in all the following experiments because that represents the best trade-off between low alkalinity and high glucose electro-oxidation. Gold nanoparticles contained in the ink used to fabricate the WE of our sensors have electro-catalytical activity for glucose oxidation.[10,28] Thus, as-fabricated sensors with non-functionalized gold WE were used as a control for non-enzymatic glucose detection. CV were recorded with gold WE in 0.1 M NaOH as the electrolyte in the presence of 0, 0.5, 1, 2.5, 5 mM glucose (Fig. S4, scan rate: 100 mV s^{-1}). An anodic peak, that increases as a function of the glucose concentration, was observed at 0.15 V and attributed to the electro-oxidation of glucose by the gold nanoparticles of the sintered ink.[29,30] Therefore, a voltage V^*_b = 0.15 V was chosen in the following CA tests performed on bare gold WEs. The suitability of the identified working potential for bare and modified WE was confirmed by operating both electrodes during CA measurements at V^*_m and V^*_b (Fig. S5). It was found that in both cases the sensitivity to glucose of the modified WE is much higher than the bare gold WE. As expected, higher sensitivity to glucose was observed when both bare and modified WE work at their corresponding optimal potential (0.15 V and 0.4 V, respectively).

3.4. Glucose detection using CuO-µPs-modified IJP sensors

The commonly accepted mechanism for CuO-catalyzed electro-oxidation of glucose in alkaline environment relies on the electrochemical conversion of CuO into strong oxidizing Cu(III) species such as CuOOH or Cu(OH)4−. Such Cu(III)-based species promptly oxidize glucose into gluconolactone which is finally converted into gluconic acid by hydrolyzation (Fig. 4A).[31–33] This mechanism can be described by the following Equations:

1) $CuO+OH- \rightarrow CuOOH$ or $CuO + H_2O + 2OH- \rightarrow Cu(OH)^{4-} + e^-$

2) Cu(III) + glucose → gluconolactone + Cu(II)

3) Gluconolactone → gluconic acid (hydrolysis).

The CA detection of glucose using our modified electrodes is shown in Fig. 4B and Fig. S6A. The current was recorded in real time upon spiking aliquots of glucose at increasing concentrations, while a constant potential of +0.4 V was applied. Glucose concentrations from 100 nM to about 30 mM were tested. The IJP CuO-µPs glucose sensor showed a high sensitivity to glucose, generating a prompt increase of current density upon the injection of each aliquot, with a response time as low as 12 seconds (Fig. 4B, inset). A saturating behavior of the steady state current vs glucose concentration was observed (Fig. 4C), with data following a Michaelis-Menten equation: $y = V_{max}\, C/(K_d + C)$, where V_{max} represents the maximum reaction rate, C is the glucose concentration, and K_d is the Michaelis-Menten constant. A good fit to the data was achieved using the above equation (correlation coefficients, $R^2 = 0.996$), with the calculated fitting parameters $V_{max} = 5.55$ mA cm^{-2} and $K_d = 7.95$ mM. The calculated K_d value indicates that a linear behavior holds at concentrations negligible compared to ~8 mM, as actually demonstrated by the excellent linearity observed in the 3 µM – 700 µM (Fig. 4D) and 3 µM – 80 µM (Fig. S6B) regions of the calibration curve, with $R^2 = 0.985$ and 0.9985, respectively. From the linear fit in the 3 – 80 µM range, a sensitivity S = 850 µA mM^{-1} cm^{-2} and a limit of detection (LOD) of 2.99 µM were calculated. The effective glucose detection in such a low concentration range opens to analytical applications on external biofluids, such as tears, where glucose was reported in the range 13-600 µM instead of the millimolar range of blood glucose.[20,34] For this reason, we decided to focus on tear fluid as the target biofluid for the subsequent experiments

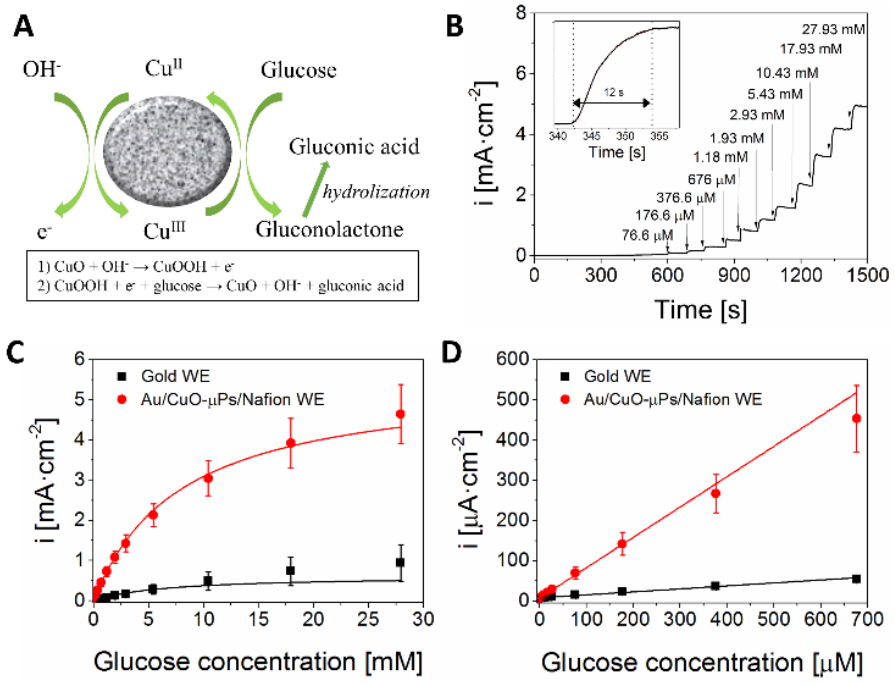

Figure 4. Amperometric detection of glucose. A) Copper-induced electro-oxidation of glucose in alkaline environment. B) CA response of the IJP CuO-µPs glucose sensor in a 0.1 M NaOH solution as a function of the glucose concentration. The inset shows a typical response time upon an aliquot addition. C) Calibration curve obtained from the CA measurements. The solid lines represent fits using the Michaelis-Menten equation. Error bars correspond to the standard deviation of the data points (n=3). D) Close up of the 3 – 700 µM region of the calibration curve.

Table 1. Comparison of the analytical performance of inkjet-printed glucose sensors.

	Electrode	Flexible	Full electrode integration	Operating potential [V]	Sensitivity [$\mu A\ mM^{-1}\ cm^{-2}$]	Linear range [mM]	Detection limit [µM]	Real sample	Ref.
Non enzymatic	Nafion/CuO-µPs/Au	√	√	+0.40	850	0.003 – 0.7	2.99	Tears	This work
	CuO-NPs/Ag	X	X	+0.60	2762.5	0.05 - 18.45	~0.5	Serum	[35]
	CuO NPs/Ag	√	X	+0.60	1424.2	0.1-15	0.3	Serum	[36]
Enzymatic	Cell. ac./GOx/PEDOT:PSS/ITO	X	X	+0.30	0.00643	0 - 55	-	-	[37]
	Wax/GOx/PB/Carb	X	X	+0.05	$50x10^3$	0.5 – 4.2	-	-	[38]
	PEDOT/GOx/AuNPs/Gr/Au	√	√	-0.2	-	0.0275-0.220	16.7	-	[39]
	GOx/PtNPs/PANI	√	√	+0.5	-	0 - 10	2000	-	[40]
	GOx/HRP/ PEDOT:PSS/ITO	√	X	+0.30	20.5	0.59 – 1.44	270	-	[41]

GOx: glucose oxidase, PEDOT:PSS: poly(3,4-ethylenedioxythiophene):polystyrene sulfonate, ITO: Indium Tin Oxide, PB: Prussian blue, Cell. ac.: cellulose acetate, PANI: polyaniline, HRP: horseradish peroxidase

presented here. It is interesting to note that both sensitivity and LOD calculated for the functionalized electrodes in this low glucose range were about 10 times higher than those calculated for the bare Au-WEs ($S_{Au\text{-}WE}$ = 110 µA mM^{-1} cm^{-2} and $LOD_{Au\text{-}WE}$ = 130 µM, respectively). This result confirms that the functionalization of gold electrodes with CuO-µPs enhances the sensitivity to glucose during its non-enzymatic electro-oxidation. In the literature, only few IJP sensors have been applied for glucose detection, most of them relying on enzymatic detection (Table 1). The combination of versatile fabrication, full electrode integration, enzyme-free sensing, and linear response in a low concentration range represents a decisive advantage for our IJP CuO-µPs glucose sensor over similar ones presented in the literature and make it an ideal platform for rapid and cost-effective PoC analysis of tear glucose.

3.5. Effect of interferents and selectivity

In addition to glucose, body fluids usually contain several other bio-analytes that can interfere with the electro-oxidation of glucose and modify its reactivity. In order to investigate the effect of interferents, the selectivity of our modified IJP glucose sensors was studied both by CV and CA in the presence of 10 mM lactate (L), 10 mM urea (U) and 2 mM ascorbic acid (AA), that are concentrations far above their typical concentration in tear fluid (2.0–5.0 mM, 3.0–6.0 mM, and 0.61 ± 0.59 mM, respectively).[34] In Fig. 5A it can be observed that the anodic peak of the glucose electro-oxidation does not overlap with the anodic peak of any interferent studied here (scan rate: 30 mV s^{-1}). This result further corroborates the choice of an operating potential of 0.4 V for the detection of glucose, as at this potential the contribution of the electro-oxidation of the interferents is the lowest. The effect of the simultaneous presence of L, U and AA was also investigated by CV. In Fig. 5B it can be observed that L, U and AA in absence of glucose interfere with each other, resulting in a negligible signal around the electro-oxidation potential of glucose (V* = 0.4 V). When 0.5 mM glucose is added to the electrolyte containing the interferents, the characteristic anodic peak of glucose is re-established at a potential 0.4 V, confirming the selectivity of our sensor towards the detection of glucose. It can be also observed that the height of the anodic peak when glucose and interferents are simultaneously present, is 25% higher than only glucose. The increased signal from glucose electrooxidation is due to the modified electroactivity of glucose caused by the interferents (mainly AA) and should be considered when the sensor is applied to the analysis of real samples. The selectivity of the CuO-µPs sensor was finally investigated also by CA. As reported in Fig. 5C, the increase of current density caused by the addition of aliquots containing each interferent was lower than that generated upon addition of glucose.

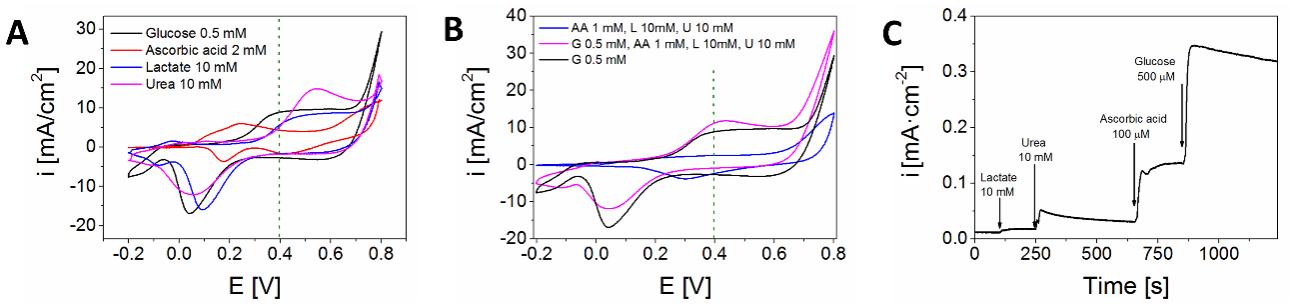

Figure 5. Effect of interferents. A) Comparison between CV measured in the presence of 0.5 mM glucose and single interferents one at a time and B) combined. The contribution of the interferents is negligible where the oxidation of glucose takes place (0.4 V). Scan rate: 30 mV s^{-1}. C) CA response of the IJP Au/CuO-µPs/Nafion sensor to several interferents.

3.6. Reproducibility, life-time and bendability

In real applications, most biosensors for health assessment are intended as disposable tools, as they are based on bio-recognition elements, such as enzymes, that lose their activity after an individual or very few uses. However, in the effort to decrease the cost of healthcare systems, innovative solutions should achieve reproducible performance over a relatively long period of time. For this reason, we characterized the reproducibility and long-term stability of our IJP CuO-µPs glucose sensor. The re-producibility of the sensor was tested by two sets of five repeated CA measurements performed in the presence of 50 µM and 300 µM glucose, respectively. In Fig. 6A it can be observed that an average current of 209.3 ± 8.2 µA cm^{-2} was reached upon spiking 300 µM glucose (I_{s300}, RSD = 3.9%), whereas an average current of 32.4 ± 3.2 µA cm^{-2} was reached upon spiking 50 µM glucose (I_{s50}, RSD = 9.9%). The little calculated RSD indicate good reproducibility of the sensors. Noteworthy, the average current values reached upon glucose spiking show a linear correlation among each other, being $I_{s300} \approx 6 * I_{s50}$, showing excellent linearity in the concentration range investigated here. The current values were also in very good agreement with the calibration curve showed in Fig. 4D, revealing the overall validity of our results. As reported in Fig. 6B, the long-term stability of our sensor was investigated over a period of 8 days in the presence of 300 µM glucose. The device response at each day was normalized with respect to the one measured at day 0, that is the day when the device was freshly functionalized and first used for measurements. The device showed a very stable response over a period longer than one week, which makes it suitable for repeated use and further lowers its effective cost. The integration of bio-sensors into flexible devices represents an added value in terms of light weight, conformability, and applicability to rolled-up production and in vivo analysis of real samples. Here, we took advantage of the intrinsic flexible nature of the thin metal films deposited by IJP to obtain a fully flexible sensing platform. Hence, we studied the ability of our sensors to withstand mechanical deformation while preserving their sensing capabilities to glucose. Fig. 6C shows how the normalized amperometric response of the CuO-µPs glucose sensor is affected by several bending cycles (curvature radius: 5 mm, inset). It can be observed that few bending cycles cause a 40 % increase of the signal, which can be probably attributed to the wrinkling of the gold electrodes that results from the stress release after the first bending cycles. Such wrinkles would increase the effective surface area of the electrode, resulting in more signal collected during the electro-oxidation of glucose. The sensor signal is retained along many tens of bending cycles, showing a 40% loss of the initial signal only after 100 bending cycles. These results show the good stability of our sensor under continuative mechanical stress.

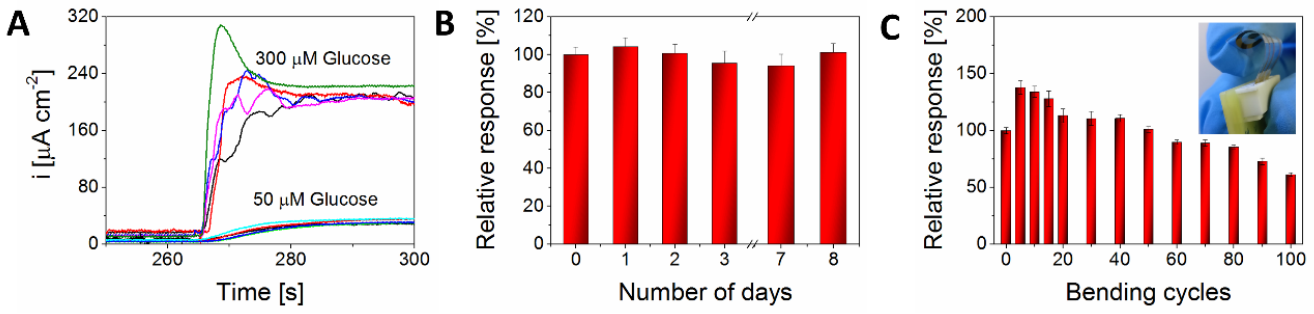

Figure 6. Reproducibility, lifetime, and bendability of IJP CuO-modified glucose sensor. A) CA response recorded upon repeated measurements in the presence of NaOH 0.1 M containing 50 µM and 300 µM glucose. B) Stability of the sensor response upon repeated measurements over more than one week (N=5). Bars are normalized with respect to the signal measured at day 0. C) Device response to repeated bending cycles (N=3). Curvature radius of bending: 5 mm. Both lifetime and bending measurements were performed in the presence of glucose 300 µM (supporting electrolyte: NaOH 0.1 M).

3.7. Determination of glucose in tear fluid

To demonstrate the applicability of the CuO-µPs glucose sensor for real samples, reflex tear samples were analyzed to determine their glucose content in real time. Two tear fluid samples were analyzed in triplicate, after being supplemented with 0 µM and 300 µM glucose, respectively. For each replicate, a 15 µL aliquot of tear fluid was injected in 1.5 mL support electrolyte (dilution 1:100) during chronoamperometric measurements (Fig. S7A). Glucose quantification was performed both using the standard addition method and recovering the actual concentration from the calibration curve, taking into account the dilution 1:100 done when spiking. In the first case, a concentration of 4.125 mM was obtained for the spiked tear sample by extrapolating the calibration line to zero response (Fig. S7B). In the second case, the average signal generated by the injection of tear fluid not supplemented with glucose corresponded to a glucose concentration of 39.4 ± 1.3 µM, according to the calibration curve in Fig. S6B (Table 2). Considering the above-mentioned dilution 1:100, the original glucose concentration in the tear aliquot is 3.94 ± 0.13 mM. As expected, the consistent results obtained by these two approaches showed tear glucose levels lower than in blood (100 mg/dL = 5.5 mM, Fig. S7C). For blood glucose analysis, a blood sample was collected simultaneously with tears using a finger pricker and quantified using a commercial glucometer and strips (AccuCheck Aviva Connect). Surprisingly, tear glucose levels relatively higher than reported in the literature were found in this work.[42,43] This could be explained considering that tear samples here were stimulated by onion vapors and collected after a meal. Indeed, glucose levels in reflex onion-induced tears have been reported to be higher than in basal tears.[44] Hence, our preliminary results on real tear samples show a trend that matches with data in the literature, and more investigations will be conducted to corroborate our findings.

Table 2. Amperometric detection of glucose in human tears.

Added glucose content (µM)	Detected content (µM)	RSD %	Recovery %
0	39.4	5.9	-
300	315.07	9.8	92.8

4. Conclusions

In this work, we report for the first time an IJP electro-chemical sensor applied for the non-enzymatic detection of glucose in tear fluid. Electrodes were printed on a flexible PET substrate by IJP and modified with CuO-µPs to detect glucose by electro-catalytic oxidation. The employment of a versatile and low-cost manufacturing technique, together with the inexpensive functionalization material led to a cost-effective sensing platform for glucose detection. The performance of the CuO-µPs glucose sensor is highest at concentration levels that match those of tear glucose. Thus, the sensor presented here is particularly well suited to non-invasively monitor the glucose level via tear analysis. The combination of several factors like versatile fabrication, full electrode integration, enzyme-free sensing, and reusability represents a decisive advantage for our sensor over similar ones presented in the literature. The IJP CuO-µPs glucose sensor offers great promises for the easy, rapid and painless monitoring of diabetes. Broader selection of electro-catalytic materials used for sensor modification will allow to develop a wide class of cheap and stable biosensors for the detection of manifold bio-analytes, like uric acid, proteins, nucleic acids, hydrogen peroxide, etc.

Appendix A. Supporting information

Supplementary data associated with this article can be found in the online version at XXX

Author Information

* Corresponding Author, Email: ssanchez@ibecbarcelona.eu
ORCID Samuel Sánchez: 0000-0002-5845-8941
† Present address: Dept of Advanced Materials for Energy Applications, Catalonia Institute for Energy Research (IREC), Sant Adrià de Besòs, Barce-lona, Spain; Instituto de Microelectronica de Barcelona, IMB-CNM (CSIC), Esfera UAB, Campus Universitat Autonoma de Barcelona, Bellaterra, Barcelona, Spain.

Acknowledgements

This work was supported by the European Research Council (ERC) Starting Grant “Lab-in-a-tube and Nano-robotics biosensors; LT-NRBS” [no. 311529] and Spanish Ministry of Economy and Competitiveness through pro-ject grant DPI2015-65401-C3-3-R MINECO/FEDER, EU. A. R. acknowledges financial support provided by the European Commission under Horizon 2020’s Marie Skłodowska-Curie Actions COFUND scheme [Grant Agreement no. 712754] and by the Severo Ochoa programme of the Spanish Ministry of Economy and Competitiveness [Grant SEV-2014-0425 (2015-2019)]. G. G. and A. M. acknowledge ICTS “NANBIOSIS”, more specifically the SU8 Unit of the CIBER in Bioengineering, Biomaterials & Nanomedicne (CIBER-BBN) at the IMB-CNM (CSIC). This work has also made use of the Spanish ICTS Network MICRONANOFABS partially supported by MEINCOM. The authors would like to thank Mrs. Felicitas Pradel for SEM-EDX investigations.

References

[1] E.T. Silva, D.E. Souto, J.T. Barragan, J.F. Giarola, A.C. Moraes, L.T. Kubota, Electrochemical biosensors in Point-of-Care devices: recent advances and future trends, ChemElectroChem. 4 (2017) 778– 794. doi:10.1002/celc.201600758.

[2] A. Moya, G. Gabriel, R. Villa, F. Javier del Campo, Inkjet-printed electrochemical sensors, Curr. Opin. Electrochem. (2017). doi:10.1016/j.coelec.2017.05.003.

[3] N. Komuro, S. Takaki, K. Suzuki, D. Citterio, Inkjet printed (bio)chemical sensing devices, Anal. Bioanal. Chem. 405 (2013) 5785–5805. doi:10.1007/s00216-013-7013-z.

[4] D. Vilela, A. Romeo, S. Sánchez, Flexible sensors for biomedical technology, Lab Chip. 16 (2016) 402–408. doi:10.1039/C5LC90136G.
[5] A.J. Bandodkar, I. Jeerapan, J. Wang, Wearable Chemical Sensors: Present Challenges and Future Prospects, ACS Sensors. 1 (2016) 464–482. doi:10.1021/acssensors.6b00250.
[6] S.K. Singh, V.M. Dhavale, R. Boukherroub, S. Kurungot, S. Szunerits, N-doped porous reduced graphene oxide as an efficient electrode material for high performance flexible solid-state supercapacitor, Appl. Mater. Today. 8 (2017) 141–149. doi:10.1016/j.apmt.2016.10.002.
[7] D. Mohapatra, S. Parida, S. Badrayyana, B.K. Singh, High performance flexible asymmetric CNO-ZnO//ZnO supercapacitor with an operating voltage of 1.8 V in aqueous medium, Appl. Mater. Today. 7 (2017) 212–221. doi:10.1016/j.apmt.2017.03.006.
[8] G. Rocchitta, A. Spanu, S. Babudieri, G. Latte, G. Madeddu, G. Galleri, S. Nuvoli, P. Bagella, M.I. Demartis, V. Fiore, R. Manetti, P.A. Serra, Enzyme Biosensors for Biomedical Applications: Strategies for Safeguarding Analytical Performances in Biological Fluids., Sensors. 16 (2016) 780–801. doi:10.3390/s16060780.
[9] D.L. Nelson, M.M. Cox, Lehninger Principles of Biochemistry, 7th ed., Macmillan, 2017.
[10] G. Wang, X. He, L. Wang, A. Gu, Y. Huang, B. Fang, B. Geng, X. Zhang, Non-enzymatic electrochemical sensing of glucose, Microchim. Acta. 180 (2013) 161–186. doi:10.1007/s00604-012-0923-1.
[11] A. Chen, S. Chatterjee, Nanomaterials based electrochemical sensors for biomedical applications, Chem. Soc. Rev. 42 (2013) 5425–5438. doi:10.1039/c3cs35518g.
[12] P. Si, Y. Huang, T. Wang, J. Ma, Nanomaterials for electrochemical non-enzymatic glucose biosensors, RSC Adv. 3 (2013) 3487–3502. doi:10.1039/c2ra22360k.
[13] X. Wang, C. Hu, H. Liu, G. Du, X. He, Y. Xi, Synthesis of CuO nanostructures and their application for nonenzymatic glucose sensing, Sensors Actuators B. 144 (2010) 220–225. doi:10.1016/j.snb.2009.09.067.
[14] H. Zhu, L. Li, W. Zhou, Z. Shao, X. Chen, D.M. Yu, Y. Choi, C.J. Lee, H.N. Alshareef, Y. Cui, Advances in non-enzymatic glucose sensors based on metal oxides, J. Mater. Chem. B. 4 (2016) 7333–7349. doi:10.1039/C6TB02037B.
[15] J. Zhang, J. Ma, S. Zhang, W. Wang, Z. Chen, A highly sensitive nonenzymatic glucose sensor based on CuO nanoparticles decorated carbon spheres, Sensors Actuators, B Chem. 211 (2015) 385–391. doi:10.1016/j.snb.2015.01.100.
[16] A. Romeo, T.S. Leung, S. Sánchez, Smart biosensors for multiplexed and fully integrated point-of-care diagnostics, Lab Chip. 16 (2016) 1957–1961. doi:10.1039/C6LC90046A.
[17] M. Zarei, Portable biosensing devices for point-of-care diagnostics: Recent developments and applications, TrAC Trends Anal. Chem. 91 (2017) 26–41. doi:10.1016/j.trac.2017.04.001.
[18] A. Tricoli, N. Nasiri, S. De, Wearable and Miniaturized Sensor Technologies for Personalized and Preventive Medicine, Adv. Funct. Mater. 27 (2017) 1–19. doi:10.1002/adfm.201605271.
[19] A.J. Bandodkar, J. Wang, Non-invasive wearable electrochemical sensors: A review, Trends Biotechnol. 32 (2014) 363–371. doi:10.1016/j.tibtech.2014.04.005.
[20] D. Pankratov, E. González-Arribas, Z. Blum, S. Shleev, Tear Based Bioelectronics, Electroanalysis. 28 (2016) 1250–1266. doi:10.1002/elan.201501116.
[21] J.T. La Belle, A. Adams, C. Lin, E. Engelschall, of a tear based glucose sensor as an alternative to self-monitoring of blood glucose, Chem. Commun. 52 (2016) 9197–9204.

doi:10.1039/C6CC03609K.
[22] H. Yao, A.J. Shum, M. Cowan, I. Lähdesmäki, B.A. Parviz, A contact lens with embedded sensor for monitoring tear glucose level, Biosens. Bioelectron. 26 (2011) 3290–3296. doi:10.1016/j.bios.2010.12.042.
[23] V. Andoralov, S. Shleev, T. Arnebrant, T. Ruzgas, Flexible micro (bio) sensors for quantitative analysis of bioanalytes in a nanovolume of human lachrymal liquid, Anal. Bioanal. Chem. 405 (2013) 3871–3879. doi:10.1007/s00216-013-6756-x.
[24] M.X. Chu, K. Miyajima, D. Takahashi, T. Arakawa, K. Sano, S.I. Sawada, H. Kudo, Y. Iwasaki, K. Akiyoshi, M. Mochizuki, K. Mitsubayashi, Soft contact lens biosensor for in situ monitoring of tear glucose as non-invasive blood sugar assessment, Talanta. 83 (2011) 960–965. doi:10.1016/j.talanta.2010.10.055.
[25] A.R. Rathmell, S.M. Bergin, Y.L. Hua, Z.Y. Li, B.J. Wiley, The growth mechanism of copper nanowires and their properties in flexible, transparent conducting films, Adv. Mater. 22 (2010) 3558–3563. doi:10.1002/adma.201000775.
[26] A. Moya, E. Sowade, F.J. del Campo, K.Y. Mitra, E. Ramon, R. Villa, R.R. Baumann, G. Gabriel, All-inkjet-printed dissolved oxygen sensors on flexible plastic substrates, Org. Electron. Physics, Mater. Appl. 39 (2016) 168–176. doi:10.1016/j.orgel.2016.10.002.
[27] X.Z. Zhang, S.D. Sun, J. Lv, L.L. Tang, C.C. Kong, X.P. Song, Z.M. Yang, Nanoparticle-aggregated CuO nanoellipsoids for high-performance non-enzymatic glucose detection, J. Mater. Chem. A. 2 (2014) 10073–10080. doi:Doi 10.1039/C4ta01005a.
[28] A.M.C. Luna, M.F.L. de Mele, A.J. Arvia, The electro-oxidation of glucose on microcolumnar gold electrodes in different neutral solutions, J. Electroanal. Chem. 323 (1992) 149–162. doi:10.1016/0022-0728(92)80008-R.
[29] S. Cho, C. Kang, Nonenzymatic Glucose Detection with Good Selectivity Against Ascorbic Acid on a Highly Porous Gold Electrode Subjected to Amalgamation Treatment, Electroanalysis. 19 (2007) 2315–2320. doi:10.1002/elan.200703982.
[30] Y. Xia, W. Huang, J. Zheng, Z. Niu, Z. Li, Nonenzymatic amperometric response of glucose on a nanoporous gold film electrode fabricated by a rapid and simple electrochemical method, Biosens. Bioelectron. 26 (2011) 3555–3561. doi:10.1016/j.bios.2011.01.044.
[31] B. Miller, Split-Ring Disk Study of the Anodic Processes at a Copper Electrode in Alkaline Solution, J. Electrochem. Soc. 116 (1969) 1675. doi:10.1149/1.2411657.
[32] Y. Xie, C.O. Huber, Electrocatalysis and amperometric detection using an electrode made of copper oxide and carbon paste, Anal. Chem. 63 (1991) 1714–1719. doi:10.1021/ac00017a012.
[33] J.M. Marioli, T. Kuwana, Electrochemical characterization of carbohydrate oxidation at copper electrodes, Electrochim. Acta. 37 (1992) 1187–1197. doi:10.1016/0013-4686(92)85055-P.
[34] N.M. Farandos, A.K. Yetisen, M.J. Monteiro, C.R. Lowe, S.H. Yun, Contact lens sensors in ocular diagnostics, Adv. Healthc. Mater. 4 (2015) 792–810. doi:10.1002/adhm.201400504.
[35] R. Ahmad, M. Vaseem, N. Tripathy, Y.B. Hahn, Wide linear-range detecting nonenzymatic glucose biosensor based on CuO nanoparticles inkjet-printed on electrodes, Anal. Chem. 85 (2013) 10448–10454. doi:10.1021/ac402925r.
[36] K.S. Bhat, R. Ahmad, J. Yoo, Y. Hahn, Fully nozzle-jet printed non-enzymatic electrode for biosensing application, J. Colloid Interface Sci. (2017). doi:https://doi.org/10.1016/j.jcis.2017.10.088.

[37] L. Setti, A. Fraleoni-Morgera, B. Ballarin, A. Filippini, D. Frascaro, C. Piana, An amperometric glucose biosensor prototype fabricated by thermal inkjet printing, Biosens. Bioelectron. 20 (2005) 2019–2026. doi:10.1016/j.bios.2004.09.022.
[38] P.-Y. Huang, Y.-C. Liao, Highly sensitive microelectrode for glucose sensing via inkjet printing technology, 2012 IEEE Sensors. (2012) 1–4. doi:10.1109/ICSENS.2012.6411582.
[39] Z. Pu, R. Wang, J. Wu, H. Yu, K. Xu, D. Li, A flexible electrochemical glucose sensor with composite nanostructured surface of the working electrode, Sensors Actuators, B Chem. 230 (2016) 801–809. doi:10.1016/j.snb.2016.02.115.
[40] E. Song, T.H. da Costa, J.-W. Choi, A chemiresistive glucose sensor fabricated by inkjet printing, Microsyst. Technol. 23 (2017) 3505–3511. doi:10.1007/s00542-016-3160-4.
[41] Y.H. Yun, B.K. Lee, J.S. Choi, S. Kim, B. Yoo, Y.S. Kim, K. Park, Y.W. Cho, A Glucose Sensor Fabricated by Piezoelectric Inkjet Printing of Conducting Polymers and Bienzymes, Anal. Sci. 27 (2011) 375–379. doi:10.2116/analsci.27.375.
[42] Q. Yan, B. Peng, G. Su, B.E. Cohan, T.C. Major, M.E. Meyerhoff, Measurement of tear glucose levels with amperometric glucose biosensor/capillary tube configuration, Anal. Chem. 83 (2011) 8341–8346. doi:10.1021/ac201700c.
[43] B. Peng, J. Lu, A.S. Balijepalli, T.C. Major, B.E. Cohan, M.E. Meyerhoff, Evaluation of enzyme-based tear glucose electrochemical sensors over a wide range of blood glucose concentrations, Biosens. Bioelectron. 49 (2013) 204–209. doi:10.1016/j.bios.2013.05.014.
[44] C.R. Taormina, J.T. Baca, S.A. Asher, J.J. Grabowski, D.N. Finegold, Analysis of Tear Glucose Concentration with Electrospray Ionization Mass Spectrometry, J. Am. Soc. Mass Spectrom. 18 (2007) 332–336. doi:10.1016/j.jasms.2006.10.002.